Psychological Medicine

cambridge.org/psm

Connectome-based prediction of eating disorder-associated symptomatology

Ximei Chen[1,*], Debo Dong[1,*], Feng Zhou[1], Xiao Gao[1], Yong Liu[1], Junjie Wang[1], Jingmin Qin[1], Yun Tian[1], Mingyue Xiao[1], Xiaofei Xu[2], Wei Li[1], Jiang Qiu[1,3], Tingyong Feng[1,4], Qinghua He[1,3], Xu Lei[1,5] and Hong Chen[1,4]

[1]Key Laboratory of Cognition and Personality, Ministry of Education, Faculty of Psychology, Southwest University, Chongqing, China; [2]School of Computing Technologies, RMIT University, Melbourne, Australia; [3]Southwest University Branch, Collaborative Innovation Center of Assessment Toward Basic Education Quality at Beijing Normal University, Chongqing, China; [4]Research Center of Psychology and Social Development, Faculty of Psychology, Southwest University, Chongqing, China and [5]Sleep and NeuroImaging Center, Faculty of Psychology, Southwest University, Chongqing, China

Abstract

Background. Despite increasing knowledge on the neuroimaging patterns of eating disorder (ED) symptoms in non-clinical populations, studies using whole-brain machine learning to identify connectome-based neuromarkers of ED symptomatology are absent. This study examined the association of connectivity within and between large-scale functional networks with specific symptomatic behaviors and cognitions using connectome-based predictive modeling (CPM).

Methods. CPM with ten-fold cross-validation was carried out to probe functional networks that were predictive of ED-associated symptomatology, including body image concerns, binge eating, and compensatory behaviors, within the discovery sample of 660 participants. The predictive ability of the identified networks was validated using an independent sample of 821 participants.

Results. The connectivity predictive of body image concerns was identified within and between networks implicated in cognitive control (frontoparietal and medial frontal), reward sensitivity (subcortical), and visual perception (visual). Crucially, the set of connections in the positive network related to body image concerns identified in one sample was generalized to predict body image concerns in an independent sample, suggesting the replicability of this effect.

Conclusions. These findings point to the feasibility of using the functional connectome to predict ED symptomatology in the general population and provide the first evidence that functional interplay among distributed networks predicts body shape/weight concerns.

Original Article

*These authors contributed equally to this work.

Cite this article: Chen X *et al* (2023). Connectome-based prediction of eating disorder-associated symptomatology. *Psychological Medicine* **53**, 5786–5799. https://doi.org/10.1017/S0033291722003026

Received: 16 February 2022
Revised: 26 June 2022
Accepted: 7 September 2022
First published online: 30 September 2022

Key words:
Body shape/weight concerns; connectome-based predictive modeling; eating disorder symptoms; resting-state functional connectivity

Author for correspondence:
Hong Chen,
E-mail: chenhg@swu.edu.cn

Introduction

Eating disorders (EDs), including anorexia nervosa (AN), bulimia nervosa (BN), and binge eating disorder (BED), are disabling, critical, and high costing mental disorders that considerably impair physical health and disrupt psychosocial functioning (Mitchison et al., 2020; Treasure, Duarte, & Schmidt, 2020). EDs are characterized by excessive concerns about body shape and weight, and symptoms of disordered eating [i.e. eating disorder symptoms (EDSs)], including dietary restriction, binge eating, and purging. Varying combinations of these EDSs occur in different EDs and across the weight spectrum, from severely underweight to obese (Bartholdy et al., 2019; Zhang et al., 2021). Crucially, subclinical EDSs, whose prevalence is particularly high (22.2–31.6%) in children and adolescents, can predict the development of full-syndrome EDs in later life (He, Cai, & Fan, 2017; Sparti, Santomauro, Cruwys, Burgess, & Harris, 2019; Stice, Gau, Rohde, & Shaw, 2017; Tanofsky-Kraff, Schvey, & Grilo, 2020). Thus, probing the underlying neural bases of EDS subtypes, especially their brain-based predictors, would be key to identifying vulnerable individuals (who are at heightened risk for dysregulated eating behaviors and associated cognitive patterns) and developing more targeted prevention strategies (Smith, Luo, & Mason, 2021).

Neurobiological alterations in brain connectivity have been demonstrated in patients with EDs (Domakonda, He, Lee, Cyr, & Marsh, 2019; Frank, Shott, Stoddard, Swindle, & Pryor, 2021; Gaudio, Wiemerslage, Brooks, & Schiöth, 2016; Haynos et al., 2021). These findings point to the key role of neurofunctional alterations involved in executive functioning, reward processing, self-referential thinking, and body/interoceptive perception in the origin and persistence of EDs. As early symptomatic behaviors (e.g. bulimic symptoms) are predictive of the later development of clinical disorders (e.g. BN; Bartholdy *et al.*, 2019; Kotler, Cohen, Davies, Pine, & Walsh, 2001) and identifying the full range of adaptive/healthy to maladaptive/

unhealthy phenomena is essential for a comprehensive understanding of the full dynamic range and means for the promotion of well-being in as many individuals as possible (for a review, see Cuthbert, 2015), it is of critical importance to investigate the neural underpinnings of EDSs in the general population. Regarding nonclinical samples (i.e. individuals without an ED diagnosis), Oliva, Morys, Horstmann, Castiello, and Begliomini (2020) found decreased resting-state functional connectivity (rsFC) between the right middle frontal gyrus (MFG) and the right insula in normal-weight binge eaters. Our recent study on young adults has shown that more frequent EDSs (e.g. bulimic symptoms) are associated with weaker intra- and inter-network rsFC (i.e. executive control, basal ganglia, and default mode networks) (Chen et al., 2021). In addition, overeating in healthy children has been found to be positively associated with rsFC within the basal ganglia network (Shapiro et al., 2019). Despite increasing knowledge about the neuroimaging patterns of EDSs in nonclinical samples, no previous study has used a whole-brain machine learning approach to examine the connectome-based neuromarkers of specific EDSs. The identification of brain-based predictors of specific symptomatic behaviors and cognitive patterns will advance our understanding of the specificity of neuromarkers of different ED-related symptomatologies.

Connectome-based predictive modeling (CPM) is a recently developed whole-brain machine learning approach for generating brain-behavior models from whole-brain functional connectivity (FC) data (i.e. 'connectomes') (Finn et al., 2015; Shen et al., 2017). Unlike traditional correlation/regression approaches, CPM with cross-validation is designed to protect against overfitting, increasing the likelihood that the identified brain-behavior relationships will be generalized in novel samples (Shen et al., 2017). As CPM is entirely data-driven and allows one-to-one mapping back to brain anatomy, it is a powerful tool for identifying complex networks subserving multifaceted behaviors – referred to as 'neural fingerprints' (Finn et al., 2015; Shen et al., 2017). Using whole-brain FC data acquired during neurocognitive task performance and at rest, CPM has been successfully used to predict attention (Rosenberg et al., 2016, 2020; Yoo et al., 2018), processing speed (Gao et al., 2020), creativity (Beaty et al., 2018), anxiety (He et al., 2021; Wang et al., 2021), perceived stress (Liu et al., 2021), personality traits (Hsu, Rosenberg, Scheinost, Constable, & Chun, 2018), and clinical outcomes (cocaine abstinence, opioid use disorder, and major depressive disorder) (Ju et al., 2020; Lichenstein, Scheinost, Potenza, Carroll, & Yip, 2021; Yip, Scheinost, Potenza, & Carroll, 2019). However, this technique remains to be used in the identification of neural fingerprints of EDSs in non-clinical conditions.

In this study, we applied the CPM with 10-fold cross-validation (10F-CV) and used whole-brain rsFC to predict individual differences in ED-associated symptomatology (i.e. body image concerns, binge eating, and compensatory behaviors) within a discovery sample of 660 participants (dataset 1). Testing and reporting performance in independent samples facilitate the evaluation of the generalizability of results and the eventual development of useful neuroimaging-based biomarkers with real-world applicability (Shen et al., 2017). Thus, we performed external validation analyses in an independent sample of 821 participants (dataset 2) to assess the predictive power of these neural models. Based on regions/networks associated with eating disturbances identified in previous resting-state functional magnetic resonance imaging (rs-fMRI) studies (Chen et al., 2021; Domakonda et al., 2019; Haynos et al., 2021; Oliva et al., 2020; Shapiro et al., 2019), we hypothesized that connectivity within and between the frontoparietal, medial frontal, subcortical, and ventral attention networks would be most predictive of individual variations in specific EDSs, especially binge eating.

Methods

Participants

Two independent undergraduate student datasets (discovery dataset: $N = 673$; validation dataset: $N = 831$) were included in this study, and all participants were recruited from the Southwest University in Chongqing, China. Participants were recruited via on-campus advertisements (e.g. posters and flyers). These two datasets comprised individuals in our ongoing project, the Behavioral Brain Research Project of Chinese Personality (BBP), which was used to examine the predictive performance of the functional connectome on disordered eating, as well as to identify connectome-based neuromarkers of specific EDSs. Psychiatric history was obtained via self-report; participants met the requirements for magnetic resonance imaging (MRI) scanning [for further details, see Supplementary Materials (SM)]. All participants in both datasets completed the same behavioral measures and underwent the same brain scanning protocols (online Supplementary Fig. S1). Information pertaining to the data collection periods [September–December 2019 (dataset 1); September–December 2020 (dataset 2)] and EDS scores for the two samples is summarized in Table 1. All participants volunteered to participate in this study without coercion and signed a written informed consent form after receiving full written and verbal explanations regarding this study prior to enrollment. Participants were paid 50 Yuan as compensation for their time. The research protocol was reviewed for compliance with the standards for the ethical treatment of human participants and approved by the Ethical Committee for Scientific Research at the university to which the authors are affiliated.

Dataset 1 was used as the discovery sample and comprised 840 participants. A total of 124 participants were excluded from analysis since they did not complete the Eating Disorder Diagnosis Scale (EDDS), and an additional 43 were excluded due to excessive head motion during scanning [i.e. with a mean framewise displacement (FD) larger than 0.2 mm and more than 10% of outlier volumes in scanning session] (see 'Head Motion Controls' section below), resulting in a final sample of 673 participants [females, 462 (68.65%); mean age, 18.51 years, standard deviation (S.D.), 1.04; range, 16–32 years]. Dataset 2 was used as the external validation sample and comprised 1122 participants. A total of 175 participants were excluded from the final data analysis due to a missing behavior index (EDDS), while another 116 participants were excluded due to severe head motion during MRI scanning. Finally, 831 participants were included in the data analysis [females, 563 (67.75%); mean age, 17.93 years, S.D., 1.04; range, 14–25 years] (online Supplementary Fig. S1).

Measures

Demographics

Information was solicited about participants' age, sex, ethnicity, highest education level, and handedness. Weight was measured using a medical body composition analyzer (M515; seca, Hamburg, Germany), and height was measured using a seca

https://doi.org/10.1017/S0033291722003026 Published online by Cambridge University Press

Table 1. Demographic information for samples and correlations between the studied variables

Samples/Measures	*Mean* (s.d.)	Range	3	4	5	6	7	8
Discovery Dataset ($N = 660$; data collection period: September–December 2019)								
1. Sex (male/female)	210/450	–	–	–	–	–	–	–
2. Ethnicity (Han/Tujia/Hmong/other)	571/16/15/58	–	–	–	–	–	–	–
3. Age (years)	18.51 (1.03)	16∼32	1					
4. Education (years)	12.49 (0.92)	10∼19	0.96***[a]	1				
5. BMI (kg/m^2)	21.10 (2.75)	14.25∼35.69	0.05[a]	0.06[a]	1			
6. Head motion (mean FD, mm)	0.09 (0.03)	0.030∼0.199	−0.04[a]	−0.04[a]	0.17***[a]	1		
7. Body image concerns	10.42 (6.87)	0∼24	0.003[b]	0.001[b]	0.48***[b]	0.13**[b]	1	
8. Binge eating frequency	1.00 (1.57)	0∼14	0.06[b]	0.06[b]	0.07[b]	0.01[b]	0.24***[b]	1
9. Compensatory behaviors	1.59 (3.05)	0∼32	0.07[b]	0.07[b]	0.17***[b]	0.03[b]	0.31***[b]	0.28***[b]
External Validation Dataset ($N = 821$; data collection period: September–December 2020)								
1. Sex (male/female)	265/556	–	–	–	–	–	–	–
2. Ethnicity (Han/Tujia/Hmong/other)	671/33/12/105	–	–	–	–	–	–	–
3. Age (years)	17.93 (1.04)	14∼25	1					
4. Education (years)	11.94 (1.04)	10∼19	0.99***[a]	1				
5. BMI (kg/m^2)	21.68 (3.14)	15.43∼35.56	−0.02[a]	−0.02[a]	1			
6. Head motion (mean FD, mm)	0.09 (0.03)	0.033∼0.201	−0.01[a]	−0.01[a]	0.17***[a]	1		
7. Body image concerns	11.19 (6.98)	0∼24	−0.11**[b]	−0.11**[b]	0.52***[b]	0.02[b]	1	
8. Binge eating frequency	1.25 (1.84)	0∼14	−0.09*[b]	−0.09*[b]	0.10**[b]	0.01[b]	0.25***[b]	1
9. Compensatory behaviors	2.23 (3.19)	0∼33	−0.04[b]	−0.04[b]	0.15***[b]	0.04[b]	0.28***[b]	0.45***[b]

s.d., standard deviation; BMI, body mass index; FD, framewise displacement.
[a]Pearson's correlation coefficients (r).
[b]Spearman's correlation coefficients (ρ).
*$p < 0.05$. **$p < 0.01$. ***$p < 0.001$.

360° stadiometer (287 dp). Body mass index (BMI) was then calculated using the seca M515.

Eating disorder-associated symptomatology scoring

The EDDS is a 22-item self-report screen that corresponds with the *Diagnostic and Statistical Manual of Mental Disorders* (4th ed.) ED diagnostic criteria (Stice, Telch, & Rizvi, 2000). This scale has high internal consistency, satisfactory test-retest reliability, excellent concordance with structured clinical interviews and convergence with validated measures of eating disturbances (e.g. weight/shape concerns and disinhibited eating), ED risk factors, and social impairment (Stice, Fisher, & Martinez, 2004, 2000). Principal components analyses of Chinese samples of each sex showed that all items loaded on one a priori factor, suggesting that the EDDS composite has a gender-equivalent univariate structure comprising all 18 items (Jackson & Chen, 2008). Validity support for the EDDS used for Chinese samples has been found for adolescent and adult samples from Chongqing (Jackson & Chen, 2010; Luo, Jackson, Niu, & Chen, 2020) and different regions of mainland China (Chen & Jackson, 2008; Jackson & Chen, 2007). In this study, we used the EDDS to evaluate three specific cognitive symptoms and maladaptive eating behaviors: body image concerns, binge eating frequency, and compensatory behaviors (i.e. purging via self-induced vomiting or laxative use, restrictive eating, and compulsive exercise). The scoring information of the sub-dimensions is shown in online Supplementary Tables S1 and S2 (SM Methods).

Following the EDDS scoring algorithm (Stice et al., 2000), 0.00% ($n = 0$) of the participants in dataset 1 ($N = 673$) met the diagnostic criteria of AN, 1.49% [$n = 10$; females, 9 (1.34%)] met the diagnostic criteria of BN, and 0.45% [$n = 3$; females, 3 (0.45%)] met the diagnostic criteria of BED. Furthermore, 0.12% [$n = 1$; females, 1 (0.12%)], 1.08% [$n = 9$; females, 6 (0.72%)], and 0.00% ($n = 0$) of the participants in dataset 2 ($N = 831$) met the diagnostic criteria of AN, BN, and BED, respectively. Therefore, it should be noted that the samples may not be entirely healthy, though none of them reported any history of psychiatry or mental disorders.

Neuroimaging data acquisition and preprocessing

All blood oxygen level-dependent (BOLD) scans were collected using a 3-T Trio scanner (Siemens Prisma, Erlangen, Germany) at the Brain Imaging Center, Southwest University. Data were obtained during an 8-min scan using rs-fMRI and a gradient echo planar imaging sequence (parameters: repetition time, 2000 ms; echo time, 30 ms; slices, 62; slice thickness, 2 mm; field of view, 224 × 224 mm^2; flip angle, 90°; resolution matrix, 112 × 112; voxel size, 2 × 2 × 2 mm^3; phase encoding direction, posterior commissure ≫ anterior commissure). Each section contained 240 volumes. High-resolution T1-weighted structural images were acquired for coregistration purposes (parameters: repetition time, 2530 ms; echo time, 2.98 ms; field of view, 256 × 256 mm^2; flip angle, 7°; base resolution, 256 × 256; slice

https://doi.org/10.1017/S0033291722003026 Published online by Cambridge University Press

per slab, 192; slice oversampling, 33.3%; voxel size, 0.5 × 0.5 × 1 mm^3; phase encoding direction, anterior commissure ≫ posterior commissure). All participants were instructed to simply rest with their eyes closed, and not to think of anything in particular. The experimenter verified that participants did not fall asleep during MRI scanning via verbal confirmation. Foam pads and earplugs were used to minimize head movement and scanning noise.

The publicly available CONN functional connectivity toolbox (version 20.b; https://www.nitrc.org/projects/conn), in conjunction with SPM12 (Wellcome Department of Cognitive Neurology, London, UK; http://www.fil.ion.ucl.ac.uk/spm), was used to perform all preprocessing steps on all collected neuroimaging data. The images of each subject were first corrected for slice timing to reduce the within-scan acquisition time differences between slices and then realigned to eliminate the influence of head motion. The realigned images were spatially normalized to the Montreal Neurological Institute (MNI) space with a resolution voxel size of 2 × 2 × 2 mm^3 (e.g. Jiang et al., 2020). Spatial smoothing was further applied with a 6-mm full-width at half-maximum Gaussian kernel (e.g. Goldfarb, Rosenberg, Seo, Constable, & Sinha, 2020). Additional denoising steps were performed for FC analysis (e.g. Hakamata et al., 2020; Yang et al., 2021). Using the anatomical component-based correction (aCompCor) method (Behzadi, Restom, Liau, & Liu, 2007; Muschelli et al., 2014), noise signals, such as signals from cerebrospinal fluid and white matter (WM) (5 principal components), and movement parameters (6 motion parameters, 6 temporal derivatives, and their squares) were removed from the images as confounds (Friston, Williams, Howard, Frackowiak, & Turner, 1996; Satterthwaite et al., 2013). Subsequently, data scrubbing was implemented to address head motion concerns. The bad time points were regarded as regressors defined as volumes with FD power >0.5 mm as well as the two succeeding volumes and one preceding volume to reduce the spillover effect of head motion (Power, Barnes, Snyder, Schlaggar, & Petersen, 2012). Linear trends of time courses were removed and a bandpass temporal filtering (0.008, 0.09 Hz) was used to remove the effects of very-low-frequency drifts and high-frequency noises.

Head motion controls

To ensure that head motion artifacts were not driving observed effects, we first adopted a widely used criterion of head motion to exclude participants if the mean FD was larger than 0.2 mm and the number of volumes with a FD >0.5 mm was more than 10% of the total number of volumes (Power et al., 2012; Yan, Wang, Zuo, & Zang, 2016; Yang et al., 2021). Accordingly, 159 participants were excluded from the entire sample due to severe head motion. Finally, in the discovery dataset (N = 673), the number of volumes with FD >0.5 mm ranged from 0 to 25, with a mean of 2.89 (the percentage of volumes with FD >0.5 mm ranged from 0% to 10%, with a mean of 1.00%). In the external validation dataset (N = 831), the number of volumes with FD >0.5 mm ranged from 0 to 25, with a mean of 3.78 (the percentage of volumes with FD >0.5 mm ranged from 0% to 10%, with a mean of 2.00%). Large amounts of head motion create robust, but spurious, patterns of connectivity. These motion patterns can artifactually increase prediction performance if motion and behavioral data are correlated (Shen et al., 2017). As such, we further assessed Spearman's correlation coefficients (ρ) between the mean FD and the observed behavior scores to verify that the behavioral measure of interest was not significantly correlated with head micromovements prior to the CPM pipeline. To further control for possible head motion confounds, we also performed a prediction analysis with the mean FD as an additional covariate (see 'Control Analyses' section below).

Functional network construction

Whole-brain FC was assessed for each subject using GRETNA (Ren et al., 2021; Wang et al., 2015). Network nodes were defined using the Shen 268-node brain atlas spanning cortical, subcortical, and cerebellar regions (Shen, Tokoglu, Papademetris, & Constable, 2013), as in previous CPM work (Gao et al., 2020; Ibrahim et al., 2021; Yip et al., 2019). For each participant, the BOLD time course of each node was extracted by taking the mean across voxels. The FC (or 'edge') was then calculated as the Pearson's correlation coefficient (r) between the mean time series of each pair of nodes. A Fisher's r-to-z transformation was then implemented to improve the normality of the correlation coefficients, resulting in a 268 × 268 symmetric connectivity matrix with 35 778 ((268 × 267)/2) edges for each participant. These edges/connections (i.e. connectivity strength) measured as Fisher-transformed correlations were used as features in the predictive models described below.

Connectome-Based predictive modeling

Ten-fold cross-validation

CPM, a recently developed technique introduced by Shen et al. (Finn et al. 2015; Rosenberg et al., 2016; Shen et al., 2017), was performed to investigate functional networks that were predictive of EDSs using a 10F-CV approach within the discovery sample (dataset 1) (e.g. Cai, Chen, Liu, Zhu, & Yu, 2020; Feng, Wang, Li, & Xu, 2019; Gao *et al.* 2020; Lu *et al.* 2019). The CPM steps included (i) feature selection, (ii) model building, and (iii) model validation (Fig. 1). These steps were implemented in MATLAB (R2017b, MathWorks). We performed the same steps for each behavioral variable (i.e. body image concerns, binge eating frequency, and compensatory behaviors). We briefly explain each step as follows. For a detailed description of the CPM technique, refer to Shen et al. (2017).

(i) Feature selection: To obtain the networks used in the prediction, Spearman's correlation coefficients were calculated between the edges and the observed behavior score. As suggested by Shen et al. (2017), we used Spearman's rank correlation rather than Pearson's correlation because the observed behavior scores in our sample did not follow a normal distribution as assessed by the Kolmogorov–Smirnov test ($p < 0.05$). We obtained ρ and p values for each edge. Next, we extracted a positive network and a negative network by selecting edges that were positively and negatively associated with the behavior scores, respectively, using a threshold of $p < 0.01$, which was widely adopted in previous CPM studies (e.g. Gao *et al.*, 2020; Liu *et al.*, 2021; Takagi *et al.*, 2018; Wang *et al.*, 2021; Zhang *et al.*, 2022). Subsequently, we summed the edge values in the positive and negative networks, respectively, to characterize the network strength (a single summary statistic) for each participant.

(ii) Model building: The network strength indices extracted from the positive and negative networks were fitted to three linear

https://doi.org/10.1017/S0033291722003026 Published online by Cambridge University Press

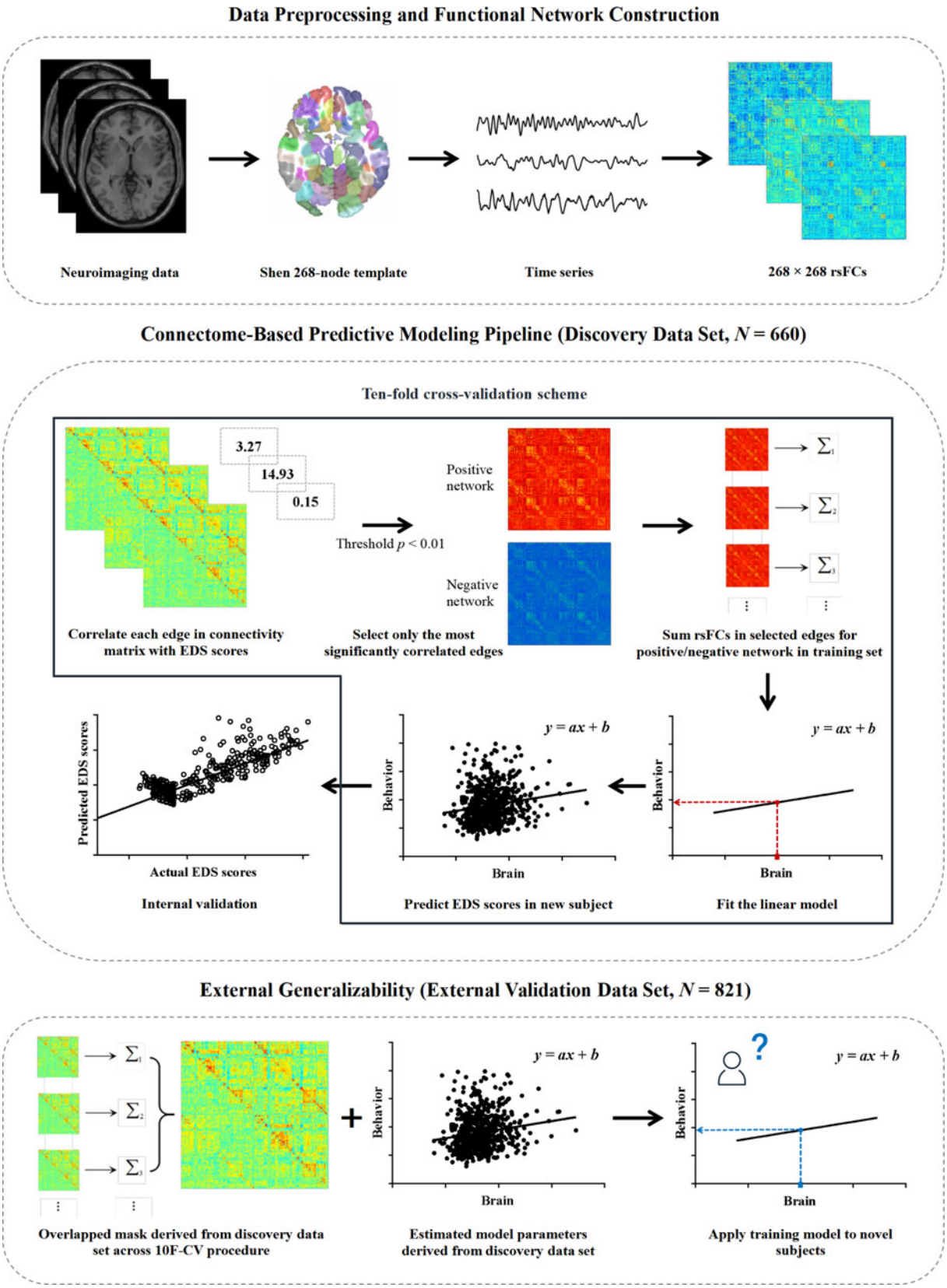

Fig. 1. The schematic flow of connectome-based predictive modeling. rsFC, resting-state functional connectivity; EDS, eating disorder symptom; 10F-CV, 10-fold cross-validation.

https://doi.org/10.1017/S0033291722003026 Published online by Cambridge University Press

regressions to generate three slopes and three intercepts. The first (i.e. positive network model) predicted the behavior scores with positive network scores, the second (i.e. negative network model) with negative network scores, and the third (i.e. combined network model) with the difference between the positive and negative network scores as an independent variable (i.e. positive score minus negative score; Greene, Gao, Scheinost, & Constable, 2018; Rosenberg et al., 2020). Specifically, participants were randomly divided into 10 subsets: nine folds (90% of participants) were used as the training set, and the remaining fold (10% of participants) was used as the testing set. The training set was used to build the linear prediction model, and the model parameters were applied to predict the behavior scores of the testing set.

(iii) Model validation: Spearman's correlation coefficient ρ and explained variance R^2 (in percentage) between the observed and predicted scores were calculated for the positive, negative, and combined network models (Poldrack, Huckins, & Varoquaux, 2020). This procedure was repeated ten times so that each subset was used as a testing set. Ten ρ and R^2 values were averaged to obtain prediction performance. The 10F-CV was repeated 100 times, and the final prediction performance was generated by averaging all the ρ and R^2 values. The significance of the model was tested using 1000 permutations.

Multiple comparisons correction

Since three predictive outcomes were tested in this study, a Bonferroni correction was applied to account for multiple testing (Scheinost et al., 2019; Yip, Kiluk, & Scheinost, 2020), with the threshold for significance was set to $p_{permu} < 0.05/3 = 0.017$ (p_{permu} values were based on 1000 permutation tests). The predictive efficacy of the network is considered statistically significant if the p_{permu} value of the network is less than 0.017.

Control analyses

Age and sex have been found to be associated with FC (Feng et al., 2018; Hsu et al., 2018), and since in-scanner motion has been identified as a prominent factor influencing FC (Horien et al., 2018; Power et al., 2014), we corrected for age, sex, and head movements (i.e. mean FD) at the model evaluation stage of CPM on the discovery dataset (i.e. when testing whether predicted scores generated by CPM significantly correlated with observed scores) (e.g. Lu et al., 2019; Ren et al., 2021). We also controlled for BMI in our predictions, given that BMI is an important factor associated with eating-related psychopathologies (Smith et al., 2021; Treasure et al., 2020) and that the current data showed significant correlations between BMI and specific EDSs (Table 1). Thus, the predictive networks used in this study were further constructed by calculating the partial Spearman's correlation between the behavior scores predicted by the CPM framework and the actual behavior scores when adjusting for the effects of age, sex, head motion, and BMI.

External validation

Testing whether the results found in one sample are applicable in another sample is an especially powerful method to assess the generalizability of CPM-based findings (Shen et al., 2017). To evaluate the external predictive validity of the set of eating symptom-related edges identified in the discovery sample, we additionally tested whether these edges were effectively predictive of EDSs in an independent external validation sample (dataset 2). The current study applied the positive and negative EDS brain networks and the model's parameters derived from the discovery dataset to the external validation dataset. Model performance using the external validation dataset was quantified as the correspondence between the predicted and actual EDS values (here, Spearman's ρ was used to account for the non-normal distribution of EDS). More details can be found in SM Methods.

Results

Behavioral data

We excluded participants with AN, BN, and BED based on the EDDS [n = 13/10 (dataset 1/2)] given that the aim of this study was the early identification in non-clinical samples. To ensure that the behavioral measure of interest was not significantly correlated with motion before the CPM process (Shen et al., 2017; see also 'Head Motion Controls' section), we calculated Spearman's correlation coefficients between head motion and behavioral variables (Table 1). The current data showed a significant association between motion (i.e. mean FD) and body image concerns ($\rho = 0.13$, $p < 0.01$); therefore, we treated mean FD as a control measure and regressed the effect of mean FD values on body image concern scores to address this concern. We used the resultant residualized body image concern scores for subsequent data analysis.

The demographic information for the two datasets and correlations between the studied variables are presented in Table 1. In the discovery sample [N = 660; females, 450 (68.18%)], females had significantly higher body image concerns ($t = 6.94$; $p < 0.001$) and binge eating frequency ($t = 2.26$; $p = 0.02$) than males. There were no significant sex differences in mean FD ($t = 0.28$; $p = 0.78$) and BMI ($t = -1.84$; $p = 0.07$), except for age (mean: females, 18.40 ± 0.82; males, 18.73 ± 1.36; $t = -3.22$; $p < 0.01$) and education level (mean: females, 12.40 ± 0.82; males, 12.69 ± 1.10; $t = -3.40$; $p < 0.01$). In the external validation sample [N = 821; females, 556 (67.72%)], females reported higher body image concerns (t = 4.32; $p < 0.001$) than males. There were no sex differences in mean FD ($t = -0.92$; $p = 0.36$), age ($t = -1.46$; $p = 0.14$), and education level ($t = -1.43$; $p = 0.15$), except for BMI (mean: females, 21.22 ± 2.69; males, 22.64 ± 3.75; $t = -5.53$; $p < 0.01$). The distributions of the demographic data of the samples are shown in online Supplementary Fig. S2.

Predictive efficacy of the model

Body image concerns[†1]

The rsFC-based predictive models showed significant correlations between the predicted and true scores (positive network: $\rho = 0.11$, $R^2 = 1.20\%$, $p_{permu} = 0.018$; negative network: $\rho = 0.11$, $R^2 = 1.50\%$, $p_{permu} = 0.010$; combined network: $\rho = 0.14$, $R^2 = 2.10\%$, $p_{permu} = 0.002$; see online Supplementary Fig. S3), with both negative and combined networks surviving a stringent Bonferroni correction for multiple comparisons (i.e. $p_{permu} < 0.05/3 = 0.017$). Similar prediction patterns were also found at the edge selection threshold of $p < 0.005$ (online Supplementary Fig. S4).

[†]The notes appear after the main text.

https://doi.org/10.1017/S0033291722003026 Published online by Cambridge University Press

Binge eating frequency

CPM failed to predict binge eating of the novel participants using rsFC features (positive network: $\rho = 0.06$, $R^2 = 0.20\%$, $p_{permu} = 0.140$; negative network: $\rho = 0.01$, $R^2 = 0.01\%$, $p_{permu} = 0.450$; combined network: $\rho = 0.04$, $R^2 = 0.14\%$, $p_{permu} = 0.227$). The binge eating models were not included in the following analyses.

Compensatory behaviors

The negative and combined networks could predict individual variations in compensatory behaviors (positive network: $\rho = 0.07$, $R^2 = 0.21\%$, $p_{permu} = 0.087$; negative network: $\rho = 0.09$, $R^2 = 0.05\%$, $p_{permu} = 0.047$; combined network: $\rho = 0.10$, $R^2 = 0.15\%$, $p_{permu} = 0.044$); however, the two networks did not survive Bonferroni correction ($p_{permu} < 0.017$) and were therefore not included in subsequent analyses.

Network neuroanatomy

Body image concerns

The spatial extent of both positive and negative networks together included 202 edges (64 positive, 138 negative; Figure 2*b*) or less than 1.5% of possible connections (i.e. the 35 778 total edges defined by the atlas used in this work; Shen et al., 2013). The highest-degree nodes (i.e. nodes with the most connections) for the positive network included a cerebellar node with connections to the temporal, prefrontal, and motorstrip nodes. The highest-degree nodes for the negative network included a subcortical node with connections to the occipital, temporal, and prefrontal nodes. Table 2 presents the top 10 nodes with the most connections contributing to the predictive models (e.g. Liu *et al.*, 2021; Lu *et al.*, 2019; Ren *et al.*, 2021; Wu *et al.*, 2022). Figure 2*a* represents networks based on the connectivity between macroscale brain regions. Brain regions are presented in an approximate anatomical order, such that longer-range connections are represented by longer lines. To facilitate the characterization of the identified body image concern networks, Fig. 2*c* summarizes the connectivity based on the number of connections within and between canonical neural networks (for example, frontoparietal and visual networks; online Supplementary Fig. S5) for the positive and negative networks, respectively. The positive body image concern network was predominantly characterized by within-network connections of the frontoparietal and medial frontal networks, and between-network connections of the frontoparietal, medial frontal, visual, and cerebellar networks. The negative and combined body image concern networks mainly comprised connections between the subcortical network and the motor/sensory, visual, and frontoparietal networks.

Control analyses

Because the current body image concern scores were adjusted for head motion (see the 'Behavioral Data' section for details), we did not control for mean FD when assessing whether the predicted body image concern scores generated by the CPM process significantly correlated with the observed body image concern scores (e.g. Wang et al., 2021). After controlling for the potential confounders of age and BMI (following the method used in prior CPM studies, e.g. Feng et al., 2019), the positive, negative, and combined networks still effectively predicted the body image concern scores; however, the predictive models failed to achieve significant correlations between the predicted and true scores when controlling for sex (online Supplementary Table S3).

External validation

This study further examined whether the positive, negative, and combined networks related to body image concerns in the discovery sample ($N = 660$) were generalized to an independent sample ($N = 821$). Edges identified in the discovery dataset as significantly related to observed behavior scores were extracted from dataset 2, and then the connectivity strength was directly entered into the final CPM to obtain the predicted behavior scores and calculate its correlation with the actual behavior scores (for further details, see SM Methods). We observed that CPM built with positive network strength could predict novel participants' body image concern scores (positive network: $\rho = 0.10$, $p = 0.028$; negative network: $\rho = 0.01$, $p = 0.88$; combined network: $\rho = 0.04$, $p = 0.25$).

Discussion

The present study applied CPM, a recently developed data-driven approach, to predict levels of ED-associated symptomatology (i.e. body image concerns, binge eating, and compensatory behaviors) in novel participants using whole-brain rsFC data. We demonstrated that inter-individual differences in body image concerns could be predicted by individual FC patterns, particularly those from the frontoparietal, medial frontal, subcortical, visual, and motor/sensory networks. Crucially, we further demonstrated that the set of connections in the positive network related to body image concerns identified in one sample generalized to predict body image concerns in an independent sample, suggesting the replicability of this effect. These novel findings point to a particularly important role of prefrontal control and subcortical reward circuits in body shape/weight concerns, which deepens our understanding of the connectome-based neuromarkers of maladaptive cognitive patterns, and may have implications for the early identification of individuals suffering from strong ED-associated symptomatology in the general population.

Major findings

Consistent with the connectome-based approach, the body image concern networks are complex and include connections between multiple, well-established neural networks (Finn et al., 2015; Rosenberg et al., 2016). The positive network included more connections within the frontoparietal and medial frontal networks, as well as more connections between the frontoparietal network and the medial frontal and visual networks (e.g. dorsolateral prefrontal cortex, MFG, frontal eye fields, and cerebellum). In contrast, the negative network included more connections between the subcortical network and the motor/sensory and visual networks (e.g. caudate, supramarginal gyrus, and secondary visual cortex). It has been demonstrated that the positive or negative feelings that individuals develop towards their bodily appearance (i.e. the affective component of body image; Cash, 2004) are related to alterations in the prefrontal cortex, and that the beliefs and mental representation of physical appearance (i.e. the cognitive component of body image) are linked to the posterior parietal areas (for reviews, see Badoud & Tsakiris, 2017; Gaudio & Quattrocchi, 2012). It is highly plausible that the abnormal engagement of frontoparietal network-mediated cognitive control (e.g. cognitive inflexibility) manifesting as elevated intra-network functional synchrony may contribute to negative thoughts and emotions regarding body image (e.g. ruminative preoccupation with body shape and fear of weight gain). This interpretation is

https://doi.org/10.1017/S0033291722003026 Published online by Cambridge University Press

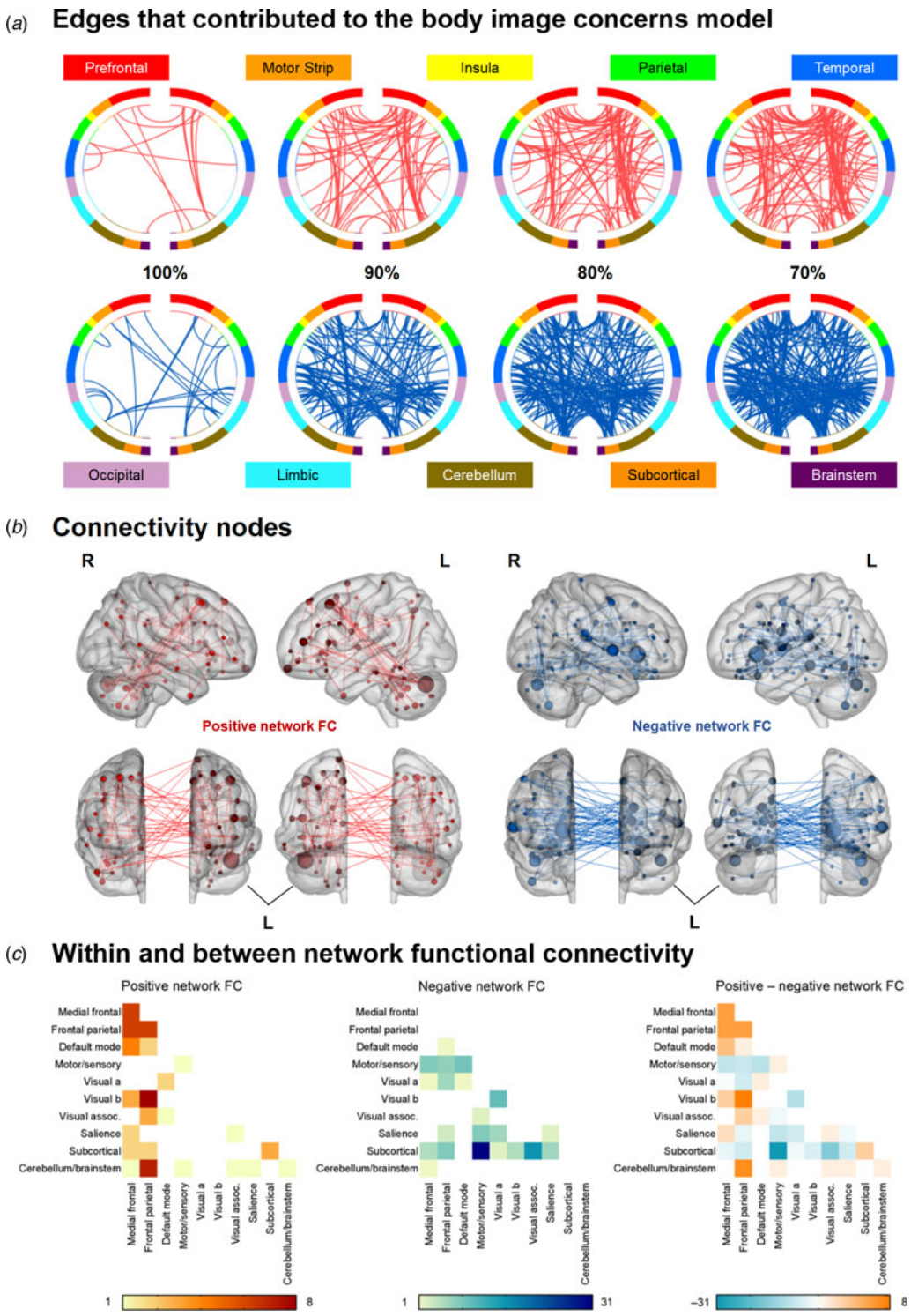

Fig. 2. Networks predicting body image concerns summarized by connectivity between macroscale brain regions and networks. (*a*) From the top, brain regions are presented in an approximate anatomical order whereby longer-range connections are represented by longer lines. The first set of plots contains edges that appeared in 100% of the 1000 predictions. To facilitate identifying brain region contributions in the model, edges that appeared in more than 90, 80, and 70% of the predictions are also shown, respectively (Horien et al., 2019; Ju et al., 2020; Rosenberg, Hsu, Scheinost, Todd Constable, & Chun, 2018). (*b*) For edges that appeared in more than 90% of the predictions, displays the positive network (red), for which stronger connectivity predicts more body image concerns and the negative network (blue), in which decreased connectivity is associated with more body image concerns. Larger spheres correspond to higher degree nodes (i.e. with more edges) contributing to the CPM model. (*c*) For edges that appeared in more than 90% of the predictions, summarizes positive and negative network anatomy based on overlap with canonical neural networks. Cells along the diagonal represent within-network connectivity and the remaining cells correspond to between-network connectivity. Color bars correspond to the total number of edges within/between each canonical neural network, with darker colors indicating a greater number of edges. The last figure shows the number of positive *v.* negative edges that correspond to different canonical neural networks, with warmer colors (orange) indicating more edges in the positive network and cooler colors (green) indicating more edges in the negative network (see online Supplementary Fig. S5 for further details on network definitions). L, left hemisphere; R, right hemisphere; FC, functional connectivity; CPM, connectome-based predictive modeling.

https://doi.org/10.1017/S0033291722003026 Published online by Cambridge University Press

Table 2. Ten nodes with the most connections contributing to the body image concerns model ($N = 660$)

No.	*K*	Node name	Network	L/R	Lobe	BA	MNI coordinates (*x*, *y*, *z*)		
Positive network[a]									
1	8	Cerebellum	Visual II	L	Cerebellum	n/a	−40.32	−74.2	−29.15
2	5	Frontal eye fields	Medial frontal	L	Prefrontal	8	−39.35	17.2	46.7
3	4	Dorsolateral Prefrontal cortex	Fronto-parietal	L	Prefrontal	46	−42.97	42.04	11.04
4	4	Frontal eye fields	Medial frontal	L	Prefrontal	8	−5.03	17.67	46.05
5	4	Middle frontal gyrus	Fronto-parietal	L	Prefrontal	10	−18.21	56.99	−14.27
6	4	Supplementary Motor cortex	Fronto-parietal	R	MotorStrip	6	25.22	12.41	49.39
7	3	Thalamus	Basal ganglia	L	Subcortical	n/a	−4.87	−10.34	5.83
8	3	Caudate	Basal ganglia	L	Subcortical	n/a	−14.6	−3.51	21.09
9	3	Cerebellum	Cerebellum	L	Cerebellum	n/a	−8.7	−50.56	−39.56
10	3	Middle occipital gyrus	Visual association	L	Parietal	7	−28.41	−62.35	40.42
Negative network									
1	14	Caudate	Basal ganglia	R	Subcortical	n/a	12.56	20.19	−0.7
2	11	Superior temporal gyrus	Motor	R	Temporal	41	59.18	−3.36	2.74
3	10	Parahippocampal gyrus	Basal ganglia	L	Limbic	36	−20.71	−30.77	−11.12
4	9	Precentral gyrus	Motor	L	MotorStrip	6	−56.98	−3.43	6.82
5	9	Cerebellum	Visual II	R	Cerebellum	n/a	39.09	−74.91	−29.7
6	7	Caudate	Basal ganglia	L	Subcortical	n/a	−12.52	11.62	8.68
7	7	Fusiform	Visual I	L	Occipital	19	−25.9	−63.14	−12.25
8	7	Supramarginal gyrus	Motor	L	Parietal	40	−42.21	−31.23	15.89
9	7	Orbitofrontal cortex	Limbic	L	Prefrontal	11	−18.22	19.05	−20.98
10	7	Supramarginal gyrus	Motor	R	Parietal	40	58	−29.28	19.53
Combined network									
1	15	Caudate	Basal ganglia	R	Subcortical	n/a	12.56	20.19	−0.7
2	11	Cerebellum	Visual II	L	Cerebellum	n/a	−40.32	−74.2	−29.15
3	11	Cerebellum	Visual II	R	Cerebellum	n/a	39.09	−74.91	−29.7
4	11	Superior temporal gyrus	Motor	R	Temporal	41	59.18	−3.36	2.74
5	10	Parahippocampal gyrus	Basal ganglia	L	Limbic	36	−20.71	−30.77	−11.12
6	9	Caudate	Basal ganglia	L	Subcortical	n/a	−14.6	−3.51	21.09
7	9	Caudate	Basal ganglia	L	Subcortical	n/a	−12.52	11.62	8.68
8	9	Precentral gyrus	Motor	L	MotorStrip	6	−56.98	−3.43	6.82
9	8	Cerebellum	n/a	R	Cerebellum	n/a	41.9	−63.98	−49.17
10	7	Thalamus	Basal ganglia	L	Subcortical	n/a	−4.87	−10.34	5.83

L, left hemisphere; R, right hemisphere; BA, Brodmann area; MNI, Montreal Neurological Institute.
Notes: These key nodes were defined as those highest in degree – the number of connections/edges the node was involved in (see also Fig. 2*b*). *K*, degree; n/a, not available.
[a]Subcortical nodes also included the right caudate ($K = 1$; network: basal ganglia; coordinates: 12.7, 12.93, 11.49), right caudate ($K = 1$; network: basal ganglia; coordinates: 12.56, 20.19, −0.7), and left caudate ($K = 2$; network: basal ganglia; coordinates: −12.52, 11.62, 8.68).

consistent with a previous study involving AN participants, which suggested that increased FC within the frontoparietal network may be related to ruminations regarding food and bodily appearance (Boehm et al., 2014). As the positive body image concern network failed to survive multiple comparisons correction, this result should be interpreted with caution. In particular, body image disturbances (BIDs), such as overestimation of body size, have been identified as core features of AN (for reviews, see Gaudio *et al.* 2016; Glashouwer, van der Veer, Adipatria, de Jong, & Vocks, 2019). Previous studies have shown that neural alterations involved in reward functions, visuospatial body processing, and integration of visual and somatosensory perceptual information in patients with AN are linked to their BIDs (Barona et al., 2019; Favaro et al., 2012; Phillipou et al., 2016). Thus, the weakened communication between the subcortical network and motor/sensory and visual networks (as indicated by lesser inter-network FC) may be reflective of an aberrant interaction between the exteroceptive representations of the body

https://doi.org/10.1017/S0033291722003026 Published online by Cambridge University Press

and reward valuation in adults with high body image concern levels (e.g. thinness-related stimuli such as pictures of underweight women are perceived by patients with BIDs as rewarding and motivating; Monteleone et al., 2018). Since comparative research on the link between negative body image (e.g. dissatisfaction, shame, and concern in relation to body image) and functional brain network organization (i.e. network-level hypotheses) is lacking, this finding should be interpreted with caution. Nonetheless, the current identification of brain-based predictors of body image concerns in non-clinical populations represents an important first step in addressing the potential role of large-scale neural networks in body image, given that existing studies mainly focus on the visual components of body image in clinical samples (for a review, see Badoud & Tsakiris, 2017). As there does not appear to be one-to-one mapping correspondence between brain regions and psychological processes (Anderson, 2014), other interpretations of our results may be possible. Additional research should be carried out to confirm that the brain-behavior associations we have observed are best explained by executive functions, reward sensitivity, and somatosensory information processing, as we have suggested.

This study expands the work in this area by examining the neural fingerprints of specific EDSs using a recently developed machine learning approach, and revealing that the functional connectome is more sensitive in characterizing individual variations of body image concerns (rather than binge eating or compensatory behaviors) in the internal validation. Possible interpretations of the results are that the relatively large and stable individual differences in body image concerns provide a rare opportunity to construct reliable brain-behavior associations; in contrast, the complexity of the etiology of compensatory behaviors and the lack of persistent negative life events that exacerbate binge eating may weaken the ability to establish an ideal model. Future studies could investigate these interesting possibilities by including some additional measurements that may capture greater individual differences (e.g. the Binge Eating Scale; Duarte, Pinto-Gouveia, & Ferreira, 2015). Meanwhile, it is worth noting that only the positive body image concern network (rather than the negative or combined networks) could predict the body image concern scores in an independent sample (in the external validation). The finding that only one of the identified networks successfully generalizes to predict the behavioral variable of interest in an external sample is not uncommon in prior CPM work (e.g. Beaty et al., 2018; Feng et al., 2019; Wang et al., 2021). The consensus from these previous studies has been that these null results are not particularly meaningful and may arise as a result of overfitting the data in the original dataset, a common pitfall of machine learning-based techniques (Belkin, Hsu, & Mitra, 2018; Ren et al., 2021). Taken together, the present study provides support for assessing external validation in addition to internal validation (here, 10F-CV) as an important step in determining the generalizability of CPM findings (Shen et al., 2017).

Our data further demonstrated that the body image concerns model failed to achieve significant correlations between the predicted and actual scores when controlling for sex, suggesting a potential sex difference in the prediction of functional networks on individual body image concern levels. Given that rsFC can be predictive of sex, and that sex effects have been observed in previous CPM studies (Greene et al., 2018; Zhang, Dougherty, Baum, White, & Michael, 2018), future studies could test the predictive power of rsFC-based CPM separately in female and male samples to reveal sex differences in the prediction of specific EDSs. Moreover, the current models showed relatively small effect sizes (e.g. Ibrahim et al., 2021). There is evidence that individualized prediction with the group-level atlas has weaker predictive power than that with an individualized template (Wang et al., 2020). It is possible that the use of a group-level atlas in our predictions overlooked subtle brain-behavior associations (Wang et al., 2021). Although increasing the sample size will help create more generalizable models and less variable prediction results, different objectives and modeling approaches invariably require different sample sizes for satisfactory performance (Scheinost et al., 2019). Therefore, the small effect sizes observed for internal and external validation could in part be due to the use of data-driven machine learning approaches, which are expected to have small effect size estimates when applied to large datasets (Yarkoni & Westfall, 2017). At the edge selection threshold of $p < 0.005$, we found that the prediction patterns of body image concerns were similar to those at the threshold of $p < 0.01$, thereby providing added confidence in the robustness of our findings (see SM Discussion for more details). The present work provides an important contribution to novel interventions intended for maladaptive cognitive symptoms and their associated conditions (e.g. obesity; Forcano, Mata, de la Torre, & Verdejo-Garcia, 2018), such as defining connectome-based targets for neuromodulation (Siddiqi et al., 2020).

Strengths, limitations, and future directions

This study has several strengths, including a considerable number of participants, the use of a recently developed whole-brain predictive modeling approach, and task-free and stable rsFC data that can provide an objective picture of whole-brain patterns of FC in individual participants and eliminate the risk of over-representation of certain regions of interest (Horien, Shen, Scheinost, & Constable, 2019; Shen et al., 2017; Sprooten et al., 2017). However, this study also has some limitations. First, we recruited only undergraduate students, given that the aim of this study was the early identification in the general population. Future studies are needed to replicate these findings in adolescents and older adults and further test whether the current predictive models can be generalized to clinical patients with EDs/BIDs. In addition, research on the neural correlates of disordered eating in pediatric populations (e.g. whether there are critical periods during which relationships between binge eating and biomarkers may emerge) is another promising direction for future studies (Smith et al., 2021). Second, although we used key inclusion criteria to ensure that participants from both datasets had no psychiatric illness or major physical health problems, the lack of mental disorder diagnosis may have some potential impact on the inference of our results. Future studies should be conducted to specifically identify and exclude individuals with psychiatric disorders (e.g. EDs, affective disorders, and schizophrenia) through the structured clinical interview for DSM-IV, and further verify the robustness of the results. Our two samples differed significantly in the number of days between rs-fMRI scan and behavioral measures, which also needs to be improved in future studies. Third, previous studies have indicated that predictive models built from task fMRI data often outperform models built from rs-fMRI data (Greene et al., 2018). Li et al. (2020) recently found that the WM functional connectome could offer a novel applicable neuromarker to explore brain-behavior relationships. Therefore, future research should compare neural fingerprints based on rsFC and FC data acquired during task performance,

https://doi.org/10.1017/S0033291722003026 Published online by Cambridge University Press

such as the food incentive delay paradigm (Simon et al., 2015). Additional studies are necessary to explore whether the WM functional connectome can predict individual variations in ED-associated symptoms. Fourth, while CPM is a data-driven technique and is therefore not well suited for testing specific regions of interest-based hypotheses, inspection of the neuroanatomy of the networks it identifies can be useful for hypothesis generation in future studies. Using a spectral dynamic causal modeling approach (Razi, Kahan, Rees, & Friston, 2015), our future hypothesis-driven research will further investigate whether and how the underlying causal interactions (i.e. intrinsic effective connectivity) between prefrontal control (top-down) and subcortical reward (bottom-up) circuits contribute to susceptibility to EDS. Finally, this study provides information on how rsFC of non-clinical population differs across EDS scores, but may not provide clinical insights regarding an actual ED/BID. Future cross-sectional studies involving multiple samples (e.g. healthy controls, binge eaters, subthreshold BED, and BED), as well as prospective cohort studies involving newly symptomatic/disordered individuals, with longitudinal follow ups to determine who goes on to develop a frank EDS/ED, will contribute to a clearer understanding of the full range of neuromarkers from non-EDs to EDs conditions.

Conclusions

This is the first attempt to predict specific EDSs at the individual level by performing CPM of rs-fMRI data. Individual body image concerns could be predicted by the functional interplay between a wide array of FCs across distributed networks, particularly those implicated in executive functioning (frontoparietal and medial frontal), reward sensitivity (subcortical), somatosensory information processing (motor/sensory), and visual perception (visual). The profile of functional connections related to body image concerns in one sample was found to successfully predict individual variations in body image concerns in an independent sample, demonstrating the replicability of this finding. The current large-sample study demonstrates the feasibility of rsFC-based individualized prediction of ED-associated symptomatology and provides novel insights into the neural mechanisms of body shape/weight concerns in non-clinical populations, which may allow for more targeted interventions for young adults who are at heightened risk for maladaptive cognitive symptoms.

Data

CPM was performed using previously validated custom MATLAB scripts, which are freely available online (https://www.nitrc.org/projects/bioimagesuite/). To promote data transparency, anonymized data that support the findings of this research are available from the corresponding author upon reasonable request. The data and code sharing adopted by the authors comply with the requirements of the funding institute and the institutional ethics approval.

Note

1. Since our predictions were exploratory and the preliminary results may advance our understanding of the nature and extent of the brain-behavior associations, we also examined the identified, marginally significant positive network in the following analyses, which may provide additional and valuable information for the early identification of high-risk individuals.

Supplementary material. The supplementary material for this article can be found at https://doi.org/10.1017/S0033291722003026.

Acknowledgements. This study was funded by National Natural Science Foundation of China (No. 31771237; No. 32200849), the Fundamental Research Funds for the Central Universities (No. SWU1709106; No. SWU2209505), and Innovative Research Project for Postgraduate Student of Chongqing (No. CYB21083). The authors would like to express their gratitude to all associated research assistants for their help with participant recruitment and data collection and thank all participants for their time and cooperation. We would also like to thank Dr Yingkai Yang (Southwest University) for additional statistical consultation. Lastly, we would like to thank the Editage (www.editage.cn) for English language editing.

Financial support. This study was funded by National Natural Science Foundation of China (No. 31771237; No. 32200849), the Fundamental Research Funds for the Central Universities (No. SWU1709106; No. SWU2209505), and Innovative Research Project for Postgraduate Student of Chongqing (No. CYB21083).

Conflicts of interest. The authors declare that they have no conflict of interest.

Ethical standards. The research protocol was reviewed for compliance with the standards for the ethical treatment of human participants and approved by the Ethical Committee for Scientific Research at the university with which the authors are affiliated.

References

Anderson, M. L. (2014). *After phrenology: Neural reuse and the interactive brain*. Cambridge, MA: MIT Press.

Badoud, D., & Tsakiris, M. (2017). From the body's viscera to the body's image: Is there a link between interoception and body image concerns? *Neuroscience and Biobehavioral Reviews*, *77*, 237–246. doi:10.1016/j.neubiorev.2017.03.017

Barona, M., Brown, M., Clark, C., Frangou, S., White, T., & Micali, N. (2019). White matter alterations in anorexia nervosa: Evidence from a voxel-based meta-analysis. *Neuroscience and Biobehavioral Reviews*, *100*, 285–295. doi:10.1016/j.neubiorev.2019.03.002

Bartholdy, S., O'Daly, O. G., Campbell, I. C., Banaschewski, T., Barker, G., & Bokde, A., … IMAGEN Consortium. (2019). Neural correlates of failed inhibitory control as an early marker of disordered eating in adolescents. *Biological Psychiatry*, *85*(11), 956–965. doi:10.1016/j.biopsych.2019.01.027

Beaty, R. E., Kenett, Y. N., Christensen, A. P., Rosenberg, M. D., Benedek, M., Chen, Q., … Silvia, P. J. (2018). Robust prediction of individual creative ability from brain functional connectivity. *Proceedings of the National Academy of Sciences of the United States of America*, *115*(5), 1087–1092. doi:10.1073/pnas.1713532115

Behzadi, Y., Restom, K., Liau, J., & Liu, T. T. (2007). A component-based noise correction method (CompCor) for BOLD and perfusion-based fMRI. *NeuroImage*, *37*(1), 90–101. doi:10.1016/j.neuroimage.2007.04.042

Belkin, M., Hsu, D. J., & Mitra, P. (2018). Overfitting or perfect fitting? Risk bounds for classification and regression rules that interpolate. In *Advances in neural information processing systems* (pp. 2300–2311). doi:10.48550/arXiv.1806.05161, https://www.researchgate.net/publication/325754503_Overfitting_or_perfect_fitting_Risk_bounds_for_classification_and_regression_rules_that_interpolate

Boehm, I., Geisler, D., King, J. A., Ritschel, F., Seidel, M., Deza Araujo, Y., … Ehrlich, S. (2014). Increased resting state functional connectivity in the fronto-parietal and default mode network in anorexia nervosa. *Frontiers in Behavioral Neuroscience*, *8*, 346. doi:10.3389/fnbeh.2014.00346

Cai, H., Chen, J., Liu, S., Zhu, J., & Yu, Y. (2020). Brain functional connectome-based prediction of individual decision impulsivity. *Cortex*, *125*, 288–298. doi:10.1016/j.cortex.2020.01.022

Cash T. F. (2004). Body image: Past, present, and future. *Body Image*, *1*(1), 1–5. doi:10.1016/S1740-1445(03)00011-1

Chen, H., & Jackson, T. (2008). Prevalence and sociodemographic correlates of eating disorder endorsements among adolescents and young adults from China. *European Eating Disorders Review*, *16*(5), 375–385. doi:10.1002/erv.837

Chen, X., Gao, X., Qin, J., Wang, C., Xiao, M., Tian, Y., … Chen, H. (2021). Resting-state functional network connectivity underlying eating disorder symptoms in healthy young adults. *NeuroImage: Clinical*, *30*, 102671. doi:10.1016/j.nicl.2021.102671

Cuthbert, B. N. (2015). Research domain criteria: Toward future psychiatric nosologies. *Dialogues in Clinical Neuroscience*, *17*(1), 89–97. doi:10.31887/DCNS.2015.17.1/bcuthbert

Domakonda, M. J., He, X., Lee, S., Cyr, M., & Marsh, R. (2019). Increased functional connectivity between ventral attention and default mode networks in adolescents with bulimia nervosa. *Journal of the American Academy of Child and Adolescent Psychiatry*, *58*(2), 232–241. doi:10.1016/j.jaac.2018.09.433

Duarte, C., Pinto-Gouveia, J., & Ferreira, C. (2015). Expanding binge eating assessment: Validity and screening value of the binge eating scale in women from the general population. *Eating Behaviors*, *18*, 41–47. doi:10.1016/j.eatbeh.2015.03.007

Favaro, A., Santonastaso, P., Manara, R., Bosello, R., Bommarito, G., Tenconi, E., & Di Salle, F. (2012). Disruption of visuospatial and somatosensory functional connectivity in anorexia nervosa. *Biological Psychiatry*, *72*(10), 864–870. doi:10.1016/j.biopsych.2012.04.025

Feng, C., Wang, L., Li, T., & Xu, P. (2019). Connectome-based individualized prediction of loneliness. *Social Cognitive and Affective Neuroscience*, *14*(4), 353–365. doi:10.1093/scan/nsz020

Feng, C., Yuan, J., Geng, H., Gu, R., Zhou, H., Wu, X., & Luo, Y. (2018). Individualized prediction of trait narcissism from whole-brain resting-state functional connectivity. *Human Brain Mapping*, *39*(9), 3701–3712. doi:10.1002/hbm.24205

Finn, E. S., Shen, X., Scheinost, D., Rosenberg, M. D., Huang, J., Chun, M. M., … Constable, R. T. (2015). Functional connectome fingerprinting: Identifying individuals using patterns of brain connectivity. *Nature Neuroscience*, *18*(11), 1664–1671. doi:10.1038/nn.4135

Forcano, L., Mata, F., de la Torre, R., & Verdejo-Garcia, A. (2018). Cognitive and neuromodulation strategies for unhealthy eating and obesity: Systematic review and discussion of neurocognitive mechanisms. *Neuroscience and Biobehavioral Reviews*, *87*, 161–191. doi:10.1016/j.neubiorev.2018.02.003

Frank, G., Shott, M. E., Stoddard, J., Swindle, S., & Pryor, T. L. (2021). Association of brain reward response with body mass index and ventral striatal-hypothalamic circuitry among young women with eating disorders. *JAMA Psychiatry*, *78*(10), 1123–1133. doi:10.1001/jamapsychiatry.2021.1580

Friston, K. J., Williams, S., Howard, R., Frackowiak, R. S., & Turner, R. (1996). Movement-related effects in fMRI time-series. *Magnetic Resonance in Medicine*, *35*(3), 346–355. doi:10.1002/mrm.1910350312

Gao, M., Wong, C., Huang, H., Shao, R., Huang, R., Chan, C., & Lee, T. (2020). Connectome-based models can predict processing speed in older adults. *NeuroImage*, *223*, 117290. doi:10.1016/j.neuroimage.2020.117290

Gaudio, S., & Quattrocchi, C. C. (2012). Neural basis of a multidimensional model of body image distortion in anorexia nervosa. *Neuroscience and Biobehavioral Reviews*, *36*(8), 1839–1847. doi:10.1016/j.neubiorev.2012.05.003

Gaudio, S., Wiemerslage, L., Brooks, S. J., & Schiöth, H. B. (2016). A systematic review of resting-state functional-MRI studies in anorexia nervosa: Evidence for functional connectivity impairment in cognitive control and visuospatial and body-signal integration. *Neuroscience and Biobehavioral Reviews*, *71*, 578–589. doi:10.1016/j.neubiorev.2016.09.032

Glashouwer, K. A., van der Veer, R., Adipatria, F., de Jong, P. J., & Vocks, S. (2019). The role of body image disturbance in the onset, maintenance, and relapse of anorexia nervosa: A systematic review. *Clinical Psychology Review*, *74*, 101771. doi:10.1016/j.cpr.2019.101771

Goldfarb, E. V., Rosenberg, M. D., Seo, D., Constable, R. T., & Sinha, R. (2020). Hippocampal seed connectome-based modeling predicts the feeling of stress. *Nature Communications*, *11*(1), 2650. doi:10.1038/s41467-020-16492-2

Greene, A. S., Gao, S., Scheinost, D., & Constable, R. T. (2018). Task-induced brain state manipulation improves prediction of individual traits. *Nature Communications*, *9*(1), 2807. doi:10.1038/s41467-018-04920-3

Hakamata, Y., Mizukami, S., Izawa, S., Moriguchi, Y., Hori, H., Kim, Y., … Tagaya, H. (2020). Basolateral amygdala connectivity with subgenual anterior cingulate cortex represents enhanced fear-related memory encoding in anxious humans. *Biological Psychiatry: Cognitive Neuroscience and Neuroimaging*, *5*(3), 301–310. doi:10.1016/j.bpsc.2019.11.008

Haynos, A. F., Camchong, J., Pearson, C. M., Lavender, J. M., Mueller, B. A., Peterson, C. B., … Lim, K. O. (2021). Resting-state hypoconnectivity of reward networks in binge eating disorder. *Cerebral Cortex*, *31*(5), 2494–2504. doi:10.1093/cercor/bhaa369

He, J., Cai, Z., & Fan, X. (2017). Prevalence of binge and loss of control eating among children and adolescents with overweight and obesity: An exploratory meta-analysis. *International Journal of Eating Disorders*, *50*(2), 91–103. doi:10.1002/eat.22661

He, L., Wei, D., Yang, F., Zhang, J., Cheng, W., Feng, J., … Qiu, J. (2021). Functional connectome prediction of anxiety related to the COVID-19 pandemic. *The American Journal of Psychiatry*, *178*(6), 530–540. doi:10.1176/appi.ajp.2020.20070979

Horien, C., Noble, S., Finn, E. S., Shen, X., Scheinost, D., Constable, R. T. (2018). Considering factors affecting the connectome-based identification process: Comment on Waller et al. *NeuroImage*, *169*, 172–175. doi:10.1016/j.neuroimage.2017.12.045

Horien, C., Shen, X., Scheinost, D., & Constable, R. T. (2019). The individual functional connectome is unique and stable over months to years. *NeuroImage*, *189*, 676–687. doi:10.1016/j.neuroimage.2019.02.002

Hsu, W. T., Rosenberg, M. D., Scheinost, D., Constable, R. T., & Chun, M. M. (2018). Resting-state functional connectivity predicts neuroticism and extraversion in novel individuals. *Social Cognitive and Affective Neuroscience*, *13*(2), 224–232. doi:10.1093/scan/nsy002

Ibrahim, K., Noble, S., He, G., Lacadie, C., Crowley, M. J., McCarthy, G., … Sukhodolsky, D. G. (2021). Large-scale functional brain networks of maladaptive childhood aggression identified by connectome-based predictive modeling. *Molecular Psychiatry*, *27*(2), 985–999. doi:10.1038/s41380-021-01317-5

Jackson, T., & Chen, H. (2007). Identifying the eating disorder symptomatic in China: The role of sociocultural factors and culturally defined appearance concerns. *Journal of Psychosomatic Research*, *62*(2), 241–249. doi:10.1016/j.jpsychores.2006.09.010

Jackson, T., & Chen, H. (2008). Predicting changes in eating disorder symptoms among adolescents in China: An 18-month prospective study. *Journal of Clinical Child and Adolescent Psychology*, *37*(4), 874–885. doi:10.1080/15374410802359841

Jackson, T., & Chen, H. (2010). Sociocultural experiences of bulimic and non-bulimic adolescents in a school-based Chinese sample. *Journal of Abnormal Child Psychology*, *38*(1), 69–76. doi:10.1007/s10802-009-9350-0

Jiang, R., Calhoun, V. D., Fan, L., Zuo, N., Jung, R., Qi, S., … Sui, J. (2020). Gender differences in connectome-based predictions of individualized intelligence quotient and sub-domain scores. *Cerebral Cortex*, *30*(3), 888–900. doi:10.1093/cercor/bhz134

Ju, Y., Horien, C., Chen, W., Guo, W., Lu, X., Sun, J., … Li, L. (2020). Connectome-based models can predict early symptom improvement in major depressive disorder. *Journal of Affective Disorders*, *273*, 442–452. doi:10.1016/j.jad.2020.04.028

Kotler, L. A., Cohen, P., Davies, M., Pine, D. S., & Walsh, B. T. (2001). Longitudinal relationships between childhood, adolescent, and adult eating disorders. *Journal of the American Academy of Child and Adolescent Psychiatry*, *40*(12), 1434–1440. doi:10.1097/00004583-200112000-00014

Li, J., Biswal, B. B., Meng, Y., Yang, S., Duan, X., Cui, Q., … Liao, W. (2020). A neuromarker of individual general fluid intelligence from the white-matter functional connectome. *Translational Psychiatry*, *10*(1), 147. doi:10.1038/s41398-020-0829-3

Lichenstein, S. D., Scheinost, D., Potenza, M. N., Carroll, K. M., & Yip, S. W. (2021). Dissociable neural substrates of opioid and cocaine use identified via connectome-based modelling. *Molecular Psychiatry*, *26*(8), 4383–4393. doi:10.1038/s41380-019-0586-y

Liu, P., Yang, W., Zhuang, K., Wei, D., Yu, R., Huang, X., & Qiu, J. (2021). The functional connectome predicts feeling of stress on regular days and during the COVID-19 pandemic. *Neurobiology of Stress*, *14*, 100285. doi:10.1016/j.ynstr.2020.100285

Lu, X., Li, T., Xia, Z., Zhu, R., Wang, L., Luo, Y. J., … Krueger, F. (2019). Connectome-based model predicts individual differences in propensity to trust. *Human Brain Mapping*, *40*(6), 1942–1954. doi:10.1002/hbm.24503

Luo, Y.-J., Jackson, T., Niu, G.-F., & Chen, H. (2020). Effects of gender and appearance comparisons on associations between media-based appearance pressure and disordered eating: Testing a moderated mediation model. *Sex Roles*, *82*, 293–305. doi:10.1007/s11199-019-01058-4

Mitchison, D., Mond, J., Bussey, K., Griffiths, S., Trompeter, N., Lonergan, A., … Hay, P. (2020). DSM-5 full syndrome, other specified, and unspecified eating disorders in Australian adolescents: Prevalence and clinical significance. *Psychological Medicine*, *50*(6), 981–990. doi:10.1017/S0033291719000898

Monteleone, A. M., Castellini, G., Volpe, U., Ricca, V., Lelli, L., Monteleone, P., & Maj, M. (2018). Neuroendocrinology and brain imaging of reward in eating disorders: A possible key to the treatment of anorexia nervosa and bulimia nervosa. *Progress in Neuro-Psychopharmacology & Biological Psychiatry*, *80*, 132–142. doi:10.1016/j.pnpbp.2017.02.020

Muschelli, J., Nebel, M. B., Caffo, B. S., Barber, A. D., Pekar, J. J., & Mostofsky, S. H. (2014). Reduction of motion-related artifacts in resting state fMRI using aCompCor. *NeuroImage*, *96*, 22–35. doi:10.1016/j.neuroimage.2014.03.028

Oliva, R., Morys, F., Horstmann, A., Castiello, U., & Begliomini, C. (2020). Characterizing impulsivity and resting-state functional connectivity in normal-weight binge eaters. *International Journal of Eating Disorders*, *53* (3), 478–488. doi:10.1002/eat.23212

Phillipou, A., Abel, L. A., Castle, D. J., Hughes, M. E., Nibbs, R. G., Gurvich, C., & Rossell, S. L. (2016). Resting-state functional connectivity in anorexia nervosa. *Psychiatry Research: Neuroimaging*, *251*, 45–52. doi:10.1016/j.pscychresns.2016.04.008

Poldrack, R. A., Huckins, G., & Varoquaux, G. (2020). Establishment of best practices for evidence for prediction: A review. *JAMA Psychiatry*, *77*(5), 534–540. doi:10.1001/jamapsychiatry.2019.3671

Power, J. D., Barnes, K. A., Snyder, A. Z., Schlaggar, B. L., & Petersen, S. E. (2012). Spurious but systematic correlations in functional connectivity MRI networks arise from subject motion. *NeuroImage*, *59*(3), 2142–2154. doi:10.1016/j.neuroimage.2011.10.018

Power, J. D., Mitra, A., Laumann, T. O., Snyder, A. Z., Schlaggar, B. L., & Petersen, S. E. (2014). Methods to detect, characterize, and remove motion artifact in resting state fMRI. *NeuroImage*, *84*, 320–341. doi:10.1016/j.neuroimage.2013.08.048

Razi, A., Kahan, J., Rees, G., & Friston, K. J. (2015). Construct validation of a DCM for resting state fMRI. *NeuroImage*, *106*, 1–14. doi:10.1016/j.neuroimage.2014.11.027

Ren, Z., Daker, R. J., Shi, L., Sun, J., Beaty, R. E., Wu, X., … Qiu, J. (2021). Connectome-based predictive modeling of creativity anxiety. *NeuroImage*, *225*, 117469. doi:10.1016/j.neuroimage.2020.117469

Rosenberg, M. D., Finn, E. S., Scheinost, D., Papademetris, X., Shen, X., Constable, R. T., & Chun, M. M. (2016). A neuromarker of sustained attention from whole-brain functional connectivity. *Nature Neuroscience*, *19*(1), 165–171. doi:10.1038/nn.4179

Rosenberg, M. D., Hsu, W. T., Scheinost, D., Todd Constable, R., & Chun, M. M. (2018). Connectome-based models predict separable components of attention in novel individuals. *Journal of Cognitive Neuroscience*, *30*(2), 160–173. doi:10.1162/jocn_a_01197

Rosenberg, M. D., Scheinost, D., Greene, A. S., Avery, E. W., Kwon, Y. H., Finn, E. S., … Chun, M. M. (2020). Functional connectivity predicts changes in attention observed across minutes, days, and months. *Proceedings of the National Academy of Sciences of the United States of America*, *117*(7), 3797–3807. doi:10.1073/pnas.1912226117

Satterthwaite, T. D., Elliott, M. A., Gerraty, R. T., Ruparel, K., Loughead, J., Calkins, M. E., … Wolf, D. H. (2013). An improved framework for confound regression and filtering for control of motion artifact in the preprocessing of resting-state functional connectivity data. *NeuroImage*, *64*, 240–256. doi:10.1016/j.neuroimage.2012.08.052

Scheinost, D., Noble, S., Horien, C., Greene, A. S., Lake, E. M., Salehi, M., … Constable, R. T. (2019). Ten simple rules for predictive modeling of individual differences in neuroimaging. *NeuroImage*, *193*, 35–45. doi:10.1016/j.neuroimage.2019.02.057

Shapiro, A., Johnson, S. L., Sutton, B., Legget, K. T., Dabelea, D., & Tregellas, J. R. (2019). Eating in the absence of hunger in young children is related to brain reward network hyperactivity and reduced functional connectivity in executive control networks. *Pediatric Obesity*, *14*(6), e12502. doi:10.1111/ijpo.12502

Shen, X., Finn, E. S., Scheinost, D., Rosenberg, M. D., Chun, M. M., Papademetris, X., & Constable, R. T. (2017). Using connectome-based predictive modeling to predict individual behavior from brain connectivity. *Nature Protocols*, *12*(3), 506–518. doi:10.1038/nprot.2016.178

Shen, X., Tokoglu, F., Papademetris, X., & Constable, R. T. (2013). Groupwise whole-brain parcellation from resting-state fMRI data for network node identification. *NeuroImage*, *82*, 403–415. doi:10.1016/j.neuroimage.2013.05.081

Siddiqi, S. H., Taylor, S. F., Cooke, D., Pascual-Leone, A., George, M. S., & Fox, M. D. (2020). Distinct symptom-specific treatment targets for circuit-based neuromodulation. *The American Journal of Psychiatry*, *177*(5), 435–446. doi:10.1176/appi.ajp.2019.19090915

Simon, J. J., Skunde, M., Wu, M., Schnell, K., Herpertz, S. C., Bendszus, M., … Friederich, H. C. (2015). Neural dissociation of food- and money-related reward processing using an abstract incentive delay task. *Social Cognitive and Affective Neuroscience*, *10*(8), 1113–1120. doi:10.1093/scan/nsu162

Smith, K. E., Luo, S., & Mason, T. B. (2021). A systematic review of neural correlates of dysregulated eating associated with obesity risk in youth. *Neuroscience and Biobehavioral Reviews*, *124*, 245–266. doi:10.1016/j.neubiorev.2021.02.013

Sparti, C., Santomauro, D., Cruwys, T., Burgess, P., & Harris, M. (2019). Disordered eating among Australian adolescents: Prevalence, functioning, and help received. *International Journal of Eating Disorders*, *52*(3), 246–254. doi:10.1002/eat.23032

Sprooten, E., Rasgon, A., Goodman, M., Carlin, A., Leibu, E., Lee, W. H., & Frangou, S. (2017). Addressing reverse inference in psychiatric neuroimaging: Meta-analyses of task-related brain activation in common mental disorders. *Human Brain Mapping*, *38*(4), 1846–1864. doi:10.1002/hbm.23486

Stice, E., Fisher, M., & Martinez, E. (2004). Eating disorder diagnostic scale: Additional evidence of reliability and validity. *Psychological Assessment*, *16*(1), 60–71. doi:10.1037/1040-3590.16.1.60

Stice, E., Gau, J. M., Rohde, P., & Shaw, H. (2017). Risk factors that predict future onset of each DSM-5 eating disorder: Predictive specificity in high-risk adolescent females. *Journal of Abnormal Psychology*, *126*(1), 38–51. doi:10.1037/abn0000219

Stice, E., Telch, C. F., & Rizvi, S. L. (2000). Development and validation of the eating disorder diagnostic scale: A brief self-report measure of anorexia, bulimia, and binge-eating disorder. *Psychological Assessment*, *12*(2), 123–131. doi:10.1037//1040-3590.12.2.123

Takagi, Y., Sakai, Y., Abe, Y., Nishida, S., Harrison, B. J., Martínez-Zalacaín, I., … Tanaka, S. C. (2018). A common brain network among state, trait, and pathological anxiety from whole-brain functional connectivity. *NeuroImage*, *172*, 506–516. doi:10.1016/j.neuroimage.2018.01.080

Tanofsky-Kraff, M., Schvey, N. A., & Grilo, C. M. (2020). A developmental framework of binge-eating disorder based on pediatric loss of control eating. *The American Psychologist*, *75*(2), 189–203. doi:10.1037/amp0000592

Treasure, J., Duarte, T. A., & Schmidt, U. (2020). Eating disorders. *The Lancet*, *395*(10227), 899–911. doi:10.1016/S0140-6736(20)30059-3

Wang, D., Li, M., Wang, M., Schoeppe, F., Ren, J., Chen, H., … Liu, H. (2020). Individual-specific functional connectivity markers track dimensional and categorical features of psychotic illness. *Molecular Psychiatry*, *25*(9), 2119–2129. doi:10.1038/s41380-018-0276-1

Wang, J., Wang, X., Xia, M., Liao, X., Evans, A., & He, Y. (2015). GRETNA: A graph theoretical network analysis toolbox for imaging connectomics. *Frontiers in Human Neuroscience*, *9*, 386. doi:10.3389/fnhum.2015.00386

Wang, Z., Goerlich, K. S., Ai, H., Aleman, A., Luo, Y. J., & Xu, P. (2021). Connectome-based predictive modeling of individual anxiety. *Cerebral Cortex*, *31*(6), 3006–3020. doi:10.1093/cercor/bhaa407

Wu, X., Yang, Q., Xu, C., Huo, H., Seger, C. A., Peng, Z., & Chen, Q. (2022). Connectome-based predictive modeling of compulsion in obsessive-compulsive disorder. *Cerebral Cortex*, Advance online publication. doi:10.1093/cercor/bhac145

Yan, C. G., Wang, X. D., Zuo, X. N., & Zang, Y. F. (2016). DPABI: Data processing & analysis for (Resting-state) brain imaging. *Neuroinformatics*, *14* (3), 339–351. doi:10.1007/s12021-016-9299-4

Yang, W., Zhuang, K., Liu, P., Guo, Y., Chen, Q., Wei, D., & Qiu, J. (2021). Memory suppression ability can be robustly predicted by the internetwork communication of frontoparietal control network. *Cerebral Cortex*, *31*(7), 3451–3461. doi:10.1093/cercor/bhab024

Yarkoni, T., & Westfall, J. (2017). Choosing prediction over explanation in psychology: Lessons from machine learning. *Perspectives on Psychological Science*, *12*(6), 1100–1122. doi:10.1177/1745691617693393

Yip, S. W., Kiluk, B., & Scheinost, D. (2020). Toward addiction prediction: An overview of cross-validated predictive modeling findings and considerations for future neuroimaging research. *Biological Psychiatry: Cognitive Neuroscience and Neuroimaging*, *5*(8), 748–758. doi:10.1016/j.bpsc.2019.11.001

Yip, S. W., Scheinost, D., Potenza, M. N., & Carroll, K. M. (2019). Connectome-based prediction of cocaine abstinence. *The American Journal of Psychiatry*, *176*(2), 156–164. doi:10.1176/appi.ajp.2018.17101147

Yoo, K., Rosenberg, M. D., Hsu, W. T., Zhang, S., Li, C. R., Scheinost, D., … Chun, M. M. (2018). Connectome-based predictive modeling of attention: Comparing different functional connectivity features and prediction methods across datasets. *NeuroImage*, *167*, 11–22. doi:10.1016/j.neuroimage.2017.11.010

Zhang, C., Dougherty, C. C., Baum, S. A., White, T., & Michael, A. M. (2018). Functional connectivity predicts gender: Evidence for gender differences in resting brain connectivity. *Human Brain Mapping*, *39*(4), 1765–1776. doi:10.1002/hbm.23950

Zhang, D., Zhou, L., Yang, A., Li, S., Chang, C., Liu, J., & Zhou, K. (2022). A connectome-based neuromarker of nonverbal number acuity and arithmetic skills. *Cerebral Cortex*, Advance online publication. doi:10.1093/cercor/bhac108

Zhang, Z., Robinson, L., Jia, T., Quinlan, E. B., Tay, N., Chu, C., … Desrivières, S. (2021). Development of disordered eating behaviors and comorbid depressive symptoms in adolescence: Neural and psychopathological predictors. *Biological Psychiatry*, *90*(12), 853–862. doi:10.1016/j.biopsych.2020.06.003